Proceeding Series of the Brazilian Society of Computational and Applied Mathematics, v. 12, n. 1, 2026.

Trabalho apresentado no XLIV CNMAC, Fundação Getulio Vargas - Rio de Janeiro - RJ, 2025.

Proceeding Series of the Brazilian Society of Computational and Applied Mathematics

Traveling Waves for the Newtonian Foam Displacement in Porous Media

Rosmery. V. Q. Zavala [1]
Departamento de Ciencia de la Computación - Universidad Católica San Pablo, Arequipa, Perú
Laboratorio de Matematica Aplicada (LAMAP) - UFJF, Juiz de Fora, MG
Luis F. Lozano [2], Grigori Chapiro [3]
Laboratorio de Matematica Aplicada (LAMAP) - UFJF, Juiz de Fora, MG

Abstract. This work presents an analytical study of three partial differential equations systems that describe foam flow models in porous media. The first two models consider the surfactant concentration fixed above the critical micellar concentration: First Order Kinetic model and a simplified version of the Stochastic Bubble Population balance model. A significant difference between these models is the influence of critical water saturation in the first model. The third model generalizes the second by varying the surfactant concentration and considering gas mobility that depends on the surfactant concentration. We study the traveling wave solutions of such systems using phase portrait analysis. All obtained analytical solutions are confirmed using direct numerical simulations of the system of partial differential equations. The second model is validated with experimental data.

Keywords:. Foam Flow, Porous Media, Traveling Wave, Riemann Problem

1 Introduction

Oil Recovery is commonly based on continuously injecting an auxiliary fluid through the injection well until it reaches the production well, displacing the oil in the reservoir. The definition of Enhanced Oil Recovery (EOR) intends to exclude all pressure maintenance processes, but it is not restricted to a specific phase in the reservoir's production life. Many works study models of EOR methods in the last decades [1–3, 9, 10].

Alternating water and gas (WAG) injection is one of several EOR techniques that seek to reduce the mobility of the injected fluid and thus improve oil recovery. Although this method increases oil recovery, similarly to the gas injection technique, it can still be hindered by effects such as viscous fingering formation, gravity override, and reservoir heterogeneities. An alternative is diluting surfactant in the aqueous phase and injecting such a solution alternately with the gas. So, the flow inside the porous medium generates foam by reducing gas mobility considerably, consequently improving recovery efficiency. This strategy is known as foam injection. Foam injection addresses all three causes of poor sweep efficiency mentioned above, [6].

Much research has increased broadly in foam flow through porous media due to its applications in complex processes such as oil recovery and soil remediation.

The non-Newtonian flow properties and their dependence on foam generation and coalescence make the development of physical models of foam flow in porous media challenging. Several

[1] rvquispe@ucsp.edu.pe
[2] luisfer99@gmail.com
[3] grigori.chapiro@ufjf.br

models have been developed to better understand the features of foam flow in porous media. In the literature, there are substantial experimental and numerical studies of this topic [1, 3, 9]. However, there are few works addressing the foam flow from the mathematical point of view [1, 5]. This can be attributed to the novelty of the topic and the complexity of the equations.

A promising classification of models for foam displacement in porous media is based on the variable describing the foam texture. Models can be empirical (where foam texture is defined through certain empirical relations) and mechanistic (based on bubble population balance). Empiric models are less complex and more numerically stable. However, a model that assumes that the foam immediately attains local steady-state, as the strong foam is clearly inadequate in cases where strong foam generation is in doubt. Mechanistic foam models consider a specific differential equation to describe foam texture. These models have successfully matched several laboratory experiments. From a mathematical point of view, mechanistic models describe foam generation and coalescence as a source term that depends linearly on the kinetic parameter. See [9, 13] for details.

Several experimental investigations and analytical studies point to saturation and foam texture profiles that are similar to traveling waves [1, 4, 9]. This work aims to provide analytical solutions for systems that model foam injection. We present numerical solutions and experimental data to validate analytical solutions.

2 Foam Flow Models

In all models that will be studied in the following sections, we consider that ϕ denotes the porosity, u is the superficial velocity, P_c is the capillary pressure, u_g is the superficial velocity of the gas phase, k is the permeability of the medium, k_{rw} and k_{rg} are relative permeabilities of water and gas phases, and the viscosities are given by μ_w and μ_g. The foam generation source term is Φ. The critical micelle concentration is C_{cmc}. The water saturation is S_w, the dimensionless foam texture is n_D, the gas saturation is $S_g = 1 - S_w$, and C is the surfactant concentration.

2.1 Foam Flow Models with Fixed Surfactant Concentration

Considering one-dimensional, two-phase incompressible flow in a homogeneous and saturated medium. The foam displacement with fixed surfactant concentration in a porous medium can be modeled by the following system of Partial Differential Equations (PDEs):

$$\begin{aligned} &\frac{\partial}{\partial t}(\phi\, S_w) + \frac{\partial}{\partial x}(u\, f_w) = -\frac{\partial}{\partial x}\left(f_w \lambda_g \frac{dP_c}{dS_w}\frac{\partial S_w}{\partial x}\right), \\ &\frac{\partial}{\partial t}(\phi\, S_g\, n_D) + \frac{\partial}{\partial x}(u\, f_g\, n_D) = \frac{\partial}{\partial x}\left(f_w \lambda_g \frac{dP_c}{dS_w}\frac{\partial S_w}{\partial x}\, n_D\right) + \phi S_g(\mathcal{K})(n_D^{LE} - n_D). \end{aligned} \tag{1}$$

The system (1) is used to represent the first two models: The First Order Kinetic(FOK) model [5] and the Simplification of the Stochastic Bubble Population (SSBP) model [12]. In these models, the viscosity is taken as a constant, and the gas relative permeability k_{rg} is modified by the Mobility Reduction Factor [1, 12]. For the SSBP model, inspired by [1], we correlate the gas phase mobility expressions for FOK [1] and Stochastic Bubble Population (SBP) [3, 13] models. So, we obtain the Mobility Reduction Factor (MRF) as a linear function and the viscosity constant. The functions and parameter values used in these models can be found in [1, 5] for the FOK model and in [9, 12] for the SSBP model. These models differ mainly in the source term $\Phi = \phi S_g(\mathcal{K})(n_D^{LE} - n_D)$ given in Table 1. Note that Φ in the FOK model depends on the critical water saturation (S_w^*).

DOI: 10.5540/03.2026.012.01.0342

Table 1: Foam generation source term.

FOK model [1, 5]	SSBP model [9, 12]
$\mathcal{K} = K_c$	$\mathcal{K} = K_g + K_d$
$n_D^{LE}(S_w) = \begin{cases} \tanh(A(S_w - S_w^*)), & S_w > S_w^*, \\ 0, & S_w \le S_w^*. \end{cases}$	$n_D^{LE} = \dfrac{K_g}{K_g + K_d} = cons ts.$

To study the solution of system (1), we consider the initial conditions:

$$(S_w, n_D)(x,0) = \begin{cases} (S_w^-, n_D^-), & x < 0, \\ (S_w^+, n_D^+), & x > 0. \end{cases} \tag{2}$$

2.2 Foam Flow Model with Variable Surfactant Concentration

To generalize the SSBP model [12] including surfactant concentration, we obtain

$$\begin{aligned} &\frac{\partial}{\partial t}(S_w) + \frac{\partial}{\partial x}(f_w) + \frac{\partial}{\partial x}\left(\delta f_w \lambda_g \frac{dP_c}{dS_w}\frac{\partial S_w}{\partial x}\right) = 0, \\ &\frac{\partial}{\partial t}(S_g\, n_D) + \frac{\partial}{\partial x}(f_g\, n_D) - \frac{\partial}{\partial x}\left(\delta f_w \lambda_g \frac{dP_c}{dS_w}\frac{\partial S_w}{\partial x} n_D\right) = \Phi, \\ &\frac{\partial}{\partial t}(S_w\, C) + \frac{\partial}{\partial x}(f_w\, C) + \frac{\partial}{\partial x}\left(\delta f_w \lambda_g \frac{dP_c}{dS_w}\frac{\partial S_w}{\partial x} C\right) = -\alpha\, \Phi, \end{aligned} \tag{3}$$

where

$$\Phi = \frac{L\phi}{u}(1 - S_w)(K_g + K_d)(n_D^{LE} - n_D), \qquad \delta = 1/(uL), \tag{4}$$

$$n_D^{LE}(C) = \frac{K_g\, \Psi}{K_g\, \Psi + K_d}, \qquad \Psi = \Psi(C) = \begin{cases} C(2C_{cmc} - C)/(C_{cmc})^2, & C \le C_{cmc}, \\ 1, & C > C_{cmc}. \end{cases} \tag{5}$$

The fractional flow theory functions and parameter values used in the model (3) are obtained from [9, 12]. For found a unique solution of (3), we consider the initial conditions:

$$(S_w, n_D, C)(x,0) = \begin{cases} (S_w^-, n_D^-, C^-), & x < 0, \\ (S_w^+, n_D^+, C^+), & x > 0. \end{cases} \tag{6}$$

3 Traveling Waves

To find a traveling wave solution, we consider the called *traveling variable* $\xi = x - v\,t$, and we transform the system of PDEs into a system of Ordinary Differential Equations (ODEs).

3.1 Traveling Waves for FOK and SSBP Models

Using the traveling variable $\xi = x - vt$, the following system of ODEs is obtained for the variables S_w and n_D from (1):

$$\frac{dS_w}{\partial \xi} = \frac{u[f_w - f_w^+ + v_s(S_w^+ - S_w)]}{-f_w \lambda_g \frac{dP_c}{dS_w}}, \quad \frac{dn_D}{\partial \xi} = \frac{\phi\, S_g\,(\mathcal{K})(n_D^{LE} - n_D)}{u\,(1 - f_w^+ - v_s(1 - S_w^+))}. \tag{7}$$

The left and right states given in (2) become the left and right equilibrium points of (7):

$$\lim_{\xi \to -\infty}(S_w, n_D)(\xi) = (S_w^-, n_D^-), \qquad \lim_{\xi \to +\infty}(S_w, n_D)(\xi) = (S_w^+, n_D^+). \tag{8}$$

A formula for **velocity of traveling wave** is obtained

$$v = (u/\phi)v_s, \qquad \text{with} \qquad v_s = (f_w^+ - f_w^-)/(S_w^+ - S_w^-). \tag{9}$$

3.1.1 FOK Model

For a fixed S_w^+, by varying S_w^- and the foam kinetic rate K_c, we study the eigenvalues of the Jacobian matrices associated with the vector field in (7). The parameter space $S_w^- \times K_c$ is divided into six regions, as shown in Fig. 1. In Region **I**, the left equilibrium is a saddle, and the right one is a source. In Region **II**, the left equilibrium is a source, and the right one is a saddle. In Region **III**, the left equilibrium is a complex source, and the right one is a saddle. In Region **IV**, the left equilibrium is a complex sink, and the right one is a saddle. In Region **V**, the left equilibrium is a sink, and the right one is a saddle. In Region **VI**, both the left and right equilibria are saddles. For more details, see [5].

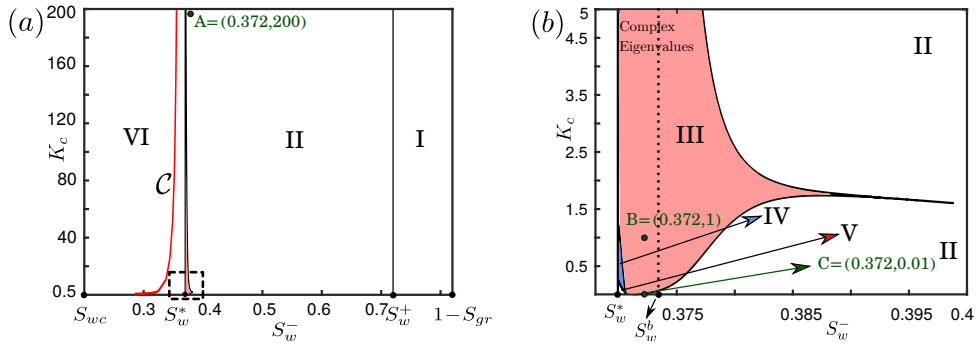

Figure 1: Classification of regions in the semi-plane $S_w \times K_c$ by equilibrium type. (a) Regions of S_w^- for $S_w^+ = 0.72$. Curve $\mathcal{C}$ represents saddle-saddle connections between left and right states. (b) Zoom near S_w^* within a small box from Fig. (a). The dotted line indicates $S_w = S_w^b$. Source [5].

3.1.2 SSBP Model

For a fixed S_w^+ by varying the value S_w^-, we study the eigenvalues of the Jacobian matrix associated with the vector field of system (7) and we describe the necessary conditions for the existence of the traveling waves. For the simplified model by [9], we arrive at a similar classification to [5]. The parameter space $S_w^- \times K_g$ is divided into regions according to the eigenvalues of the equilibria, as shown in Fig. 2. In *Region I*, the left equilibrium is a source, and the right one is a saddle. In *Region II*, the left equilibrium is a saddle, and the right one is a saddle. See [12] for more details.

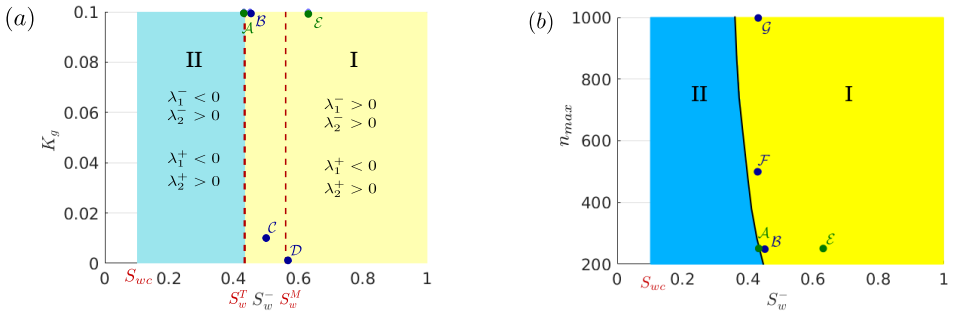

Figure 2: Regions' classification according to the equilibrium type. The points $\mathcal{B}$, $\mathcal{C}$ and $\mathcal{D}$ correspond to numerical simulations. Experimental results correspond to points $\mathcal{A}$ and $\mathcal{E}$. (a) Space $S_w^- \times K_g$ and $n_{max} = 250$ mm^{-3}. (b) Space $S_w^- \times n_{max}$ and $K_g = 0.1$. Source [12].

3.2 Traveling Waves for the Model with Surfactant Concentration

Using the traveling variable $\xi = x - v_s\, t$ in system (3), we obtain two cases:
If $(-v_s S_w^+ + f_w^+) \neq 0$,

$$\begin{aligned}
&\frac{dS_w}{d\xi} = \frac{f_w - f_w^+ + v_s(S_w^+ - S_w)}{-\delta f_w \lambda_g \frac{dP_c}{dS_w}},\\
&\frac{dC}{d\xi} = \frac{-\alpha(L\phi/u)(1-S_w)(K_g+K_d)(n_D^{LE}-n_D)}{(-v_s S_w^+ + f_w^+)},\\
&-\alpha(-v_s(1-S_w^+) + (1-f_w^+))\,(n_D - n_D^+) = (-v_s S_w^+ + f_w^+)\,(C - C^+),
\end{aligned} \tag{10}$$

If $(-v_s S_w^+ + f_w^+) = 0$, we obtain the first equation of (10) and the equations given in (11)

$$K_g\,(1-n_D)\,\Psi(C) - K_d\, n_D = 0, \;\text{ and }\; n_D = n_D^+. \tag{11}$$

The left and right states given in (6) become the left and right equilibria similarly to (8). Notice that for the system (10), the formula for the **velocity of the traveling wave** is given by v_s as defined on the right-hand side of (9) i.e. $v_s = (f_w^+ - f_w^-)/(S_w^+ - S_w^-)$.

For $C^- \neq C^+$, the formula for the **velocity of the traveling wave** can be expressed in a second way, independent of S_w^-, as observed in [11]. This formulation is used when S_w^- is not determined.

By varying C^- and C^+, we observe that the velocity of the traveling wave v_s changes, leading to different possibilities for S_w^-. Consequently, we classify the parameter space $C^- \times C^+$, as shown in Fig. 3a, based on the eigenvalues of the equilibria. For more details, see [11].

By abuse of notation, we define $f_w(S_w, C) := f_w(S_w, n_D^{LE}(C))$. Note that S_w^- is determined by the intersection of $f_w(S_w, C^-)$ and the purple line passing through the point (S_w^+, f_w^+) with slope v_s, as shown in Fig. 3b-3c. The left equilibrium is found at this intersection, and other equilibria are identified when they exist.

In regions $\mathfrak{R}^7$ and $\mathfrak{D}$, S_w^- is known, and we use the formula for v_s given in (9). In other regions, we use the alternative formula for v_s (which is independent of S_w^-) to determine the S_w^- of the left equilibrium.

In regions $\mathfrak{R}^1$, $\mathfrak{R}^2$, $\mathfrak{R}^3$, and $\mathfrak{R}^6$, there are two possible left equilibria. In regions $\mathfrak{R}^4$, $\mathfrak{R}^5$, and $\mathfrak{T}$ (when $C^- < C^+$), no valid S_w^- exists, and the left equilibrium does not exist. On curves $\mathfrak{L}$, $\mathfrak{N}$, and $\mathfrak{T}$ (when $C^- > C^+$), there is one possible left equilibrium. In region $\mathfrak{R}^7$ and curve $\mathfrak{D}$, the point (S_w^-, C_s^-) is an equilibrium for all $S_w^- \in (S_{wc}, 1 - S_{gr})$, similar to [12].

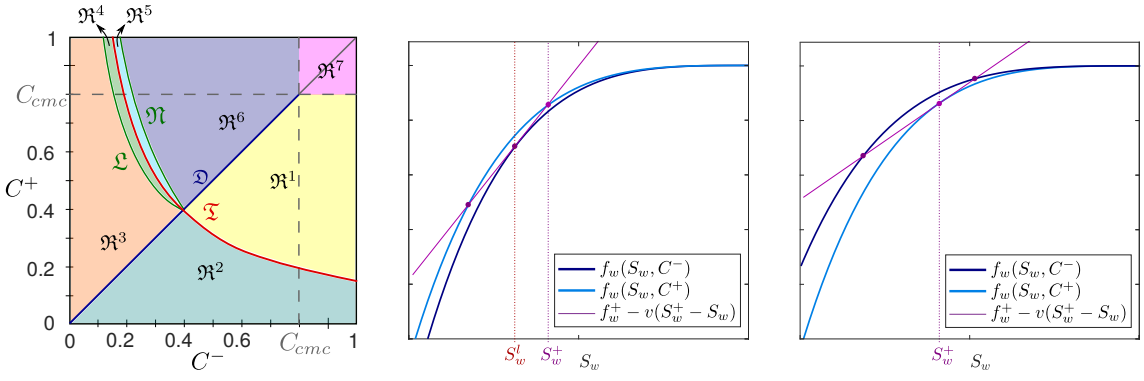

(a) Classification of $C^- \times C^+$. (b) Curve $\mathfrak{L}$. (c) Curve $\mathfrak{T}$ with $C^+ < C^-$.

Figure 3: Classification of $C^- \times C^+$ and intersection of $f_w(S_w, C^-)$ with v_s line. Source: [11].

DOI: 10.5540/03.2026.012.01.0342

4 Results and Comparative Analysis

4.1 First Order Kinetic (FOK) Model

Phase portrait analysis of system (7) for the FOK model reveals the existence of traveling wave solutions in Regions **II**, **III**, and along Curve $\mathcal{C}$ (the red curve in Fig. 1(a)), which corresponds to saddle-saddle connections between left states in Region **VI** and S_w^+. The model exhibits significant sensitivity to key parameters: small variations in K_c (order of 10^{-6}) or S_w^- (order of 10^{-2}) can produce solution divergences and lead to qualitatively different solutions, as reported in [5]. Comparative analysis shows excellent agreement with experimental (the predicted mobility decay near S_w^* as in [8]) and numerical [7] studies.

4.2 Simplified Stochastic Bubble Population (SSBP) Model

The phase portrait analysis of system (7) for the SSBP model identifies traveling wave solutions within *Region I*, where $S_w^- \in]S_w^T, S_w^+]$, and S_w^T denotes the intersection between the f_w curve and its tangent passing through (S_w^+, f_w^+). Despite its simplified formulation, the SSBP model exhibits good agreement with the complete SBP model and experimental CT scan data [9], particularly at later times, highlighting its robustness and reduced sensitivity compared to the FOK model.

4.3 Foam Flow Model with Variable Surfactant Concentration

The variable surfactant model exhibits complex solution behavior across different regions (Fig. 3a): while $\mathfrak{R}^1$ and $\mathfrak{R}^7$ (if $C^- = C^+$) admit traveling waves (consistent with SSBP model [12]), Curve $\mathfrak{T}$ (if $C^- > C^+$) reveals new regimes with higher velocities [11]. Novel solutions [11]: (i) in Region $\mathfrak{R}^2$, a traveling wave exists if the left equilibrium is a source, and (ii) along Curve $\mathfrak{D}$, the type of solution depends on S_w^- and C^+.

This model provides a unified framework that encompasses both the SSBP and, under special conditions, the FOK behavior. It offers a more realistic description for variable surfactant concentration cases and aligns with the observed transition behaviors described in [11].

5 Conclusions

We studied different systems of partial differential equations that describe the foam displacement in porous media, where the foam's dynamic behavior is assumed to be Newtonian. For the first two investigated models [5, 12], we fixed the surfactant concentration above the critical micelle concentration. Both models present identical solutions for relatively high values of injected water saturation. The second and third models [11, 12] possess similar solutions for all the values of injected water saturation since the surfactant concentration at the injection and initial conditions are equal. Hence, the solutions of all three models are similar for high values of injected water saturation and the surfactant concentration above the critical micelle concentration. For small values of injected water saturation, the models' solutions have different behaviors. A significant difference between these models is the influence of critical water saturation in the first model. This influence can induce the presence of two types of structural instabilities close to this point. Finally, from the third model, we noticed that the surfactant concentration significantly influences the foam behavior.

DOI: 10.5540/03.2026.012.01.0342

Acknowledgments

The authors gratefully acknowledge support from Shell Brasil through the project "Avançando na modelagem matemática e computacional para apoiar a implementação da tecnologia 'Foam-assisted WAG' em reservatórios do Pré-sal" (ANP 23518-4) at UFJF and the strategic importance of the support given by ANP through the R&D levy regulation. G. Chapiro was supported in part by CNPq grant 306970/2022-8, and FAPEMIG grant APQ-00206-24

References

[1] E. Ashoori, D. Marchesin, and W. R. Rossen. "Roles of transient and local equilibrium foam behavior in porous media: Traveling wave". In: **Colloids and Surfaces A: Physicochemical and Engineering Aspects** 377.1 (2011), pp. 228–242.

[2] J. B. Cedro, R. V. Quispe Zavala, M. C. Coaquira, L. F. Lozano, and G. Chapiro. "Estudo de um modelo cinético para escoamento de espuma em meios porosos". In: **CILAMCE**. Natal, Brazil, 2019.

[3] G. J. Hirasaki and J. B. Lawson. "Mechanisms of foam flow in porous media: Apparent viscosity in smooth capillaries". In: **SPE Journal** 25.2 (1985), pp. 176–190.

[4] L. F. Lozano, J. B. Cedro, R. Q. Zavala, and G. Chapiro. "How simplifying capillary effects can affect the traveling wave solution profiles of the foam flow in porous media". In: **International Journal of Non-Linear Mechanics** 139.103867 (2022).

[5] L. F. Lozano, R. Q. Zavala, and G. Chapiro. "Mathematical properties of the foam flow in porous media". In: **Computational Geosciences** 25.1 (2021), pp. 515–527.

[6] W. R. Rossen. "Foams in enhanced oil recovery". In: **Foams: Theory, measurements and applications**. Ed. by CRC Press. Vol. 57. Routledge, 1996. Chap. 11, pp. 413–464.

[7] W. R. Rossen. "Numerical challenges in foam simulation: a review". In: **Proceedings Series of SPE Annual Technical Conference and Exhibition**. New Orleans, Louisiana, USA, 2013, pp. 1–10.

[8] W. R. Rossen and P. A. Gauglitz. "Percolation theory of creation and mobilization of foams in porous media". In: **AIChE Journal** 36.8 (1990), pp. 1176–1188.

[9] M. Simjoo and P. L. J. Zitha. "Modeling of Foam Flow Using Stochastic Bubble Population Model and Experimental Validation". In: **Transport in Porous Media** 107.3 (2015), pp. 799–820.

[10] R. Q. Zavala and G. Chapiro. "Classification of the traveling wave solutions for filtration combustion considering thermal losses". In: **Combustion and Flame** 219 (2020), pp. 416–424.

[11] R. Q. Zavala, L. F. Lozano, and G. Chapiro. "Traveling wave solutions describing the foam flow in porous media for low surfactant concentration". In: **Computational Geosciences** 28.2 (2024), pp. 323–340.

[12] R. Q. Zavala, L. F. Lozano, P. L. J. Zitha, and G. Chapiro. "Analytical solution for the population-balance model describing foam displacement". In: **Transport in Porous Media** 144 (2022), pp. 211–227.

[13] P. L. J. Zitha and D. X. Du. "A New Stochastic Bubble Population Model for Foam Flow in Porous Media". In: **Transport in Porous Media** 83.3 (2010), pp. 603–621.

